



Published in final edited form as:

Hypertens Res. 2021 June ; 44(6): 628–641. doi:10.1038/s41440-021-00646-w.

Dopamine D₅ receptor-mediated decreases in mitochondrial reactive oxygen species production are cAMP and autophagy dependent

Hewang Lee^{1,2,3,4,5,6}, Xiaoliang Jiang⁷, Imran Perwaiz², Peiying Yu^{3,4,5}, Jin Wang², Ying Wang², Maik Hüttemann⁸, Robin A. Felder⁹, David R. Sibley¹⁰, Brian M. Polster¹¹, Selim Rozyyev¹, Ines Armando^{1,3,4,5}, Zhiwei Yang⁷, Peng Qu², Pedro A. Jose^{1,3,4,5,12}

¹Department of Medicine, School of Medicine & Health Sciences, George Washington University, Washington, DC, USA

²Institute of Heart and Vessel Diseases, Affiliated Second Hospital, Dalian Medical University, Dalian, China

³Division of Nephrology, Department of Medicine, School of Medicine, University of Maryland, Baltimore, MD, USA

⁴Center for Molecular Physiology Research, Children's Research Institute, Children's National Medical Center, Washington, DC, USA

⁵Department of Pediatrics, Georgetown University Medical Center, Washington, DC, USA

⁶Kidney Disease Section, National Institute of Diabetes and Digestive and Kidney Diseases, Bethesda, MD, USA

⁷Institute of Laboratory Animal Science, Chinese Academy of Medical Sciences & Comparative Medicine Center, Peking Union Medical College, Beijing, China

⁸Center for Molecular Medicine and Genetics and Cardiovascular Research Institute, School of Medicine, Wayne State University, Detroit, MI, USA

⁹Department of Pathology, University of Virginia Health Sciences Center, Charlottesville, VA, USA

¹⁰Molecular Neuropharmacology Section, National Institute of Neurological Disorders and Stroke, Bethesda, MD, USA

¹¹Department of Anesthesiology, School of Medicine, University of Maryland, Baltimore, MD, USA

¹²Department of Pharmacology and Physiology, School of Medicine & Health Sciences, George Washington University, Washington, DC, USA

[✉]Pedro A. Jose, pjose@mfa.gwu.edu.

Author contributions HL and PAJ designed the experiments. HL, XJ, IP, PY, SR, JW, and YW performed the experiments. DRS supplied the mice. HL, PY, MH, RAF, BMP, IA, ZY, PQ, and PAJ interpreted the experimental results. HL and PAJ drafted the manuscript. All authors edited, revised, and approved the final manuscript.

Supplementary information The online version contains supplementary material available at <https://doi.org/10.1038/s41440-021-00646-w>.

Conflict of interest The authors declare no competing interests.

Abstract

Overproduction of reactive oxygen species (ROS) plays an important role in the pathogenesis of hypertension. The dopamine D₅ receptor (D₅R) is known to decrease ROS production, but the mechanism is not completely understood. In HEK293 cells overexpressing D₅R, fenoldopam, an agonist of the two D₁-like receptors, D₁R and D₅R, decreased the production of mitochondria-derived ROS (mito-ROS). The fenoldopam-mediated decrease in mito-ROS production was mimicked by Sp-cAMPS but blocked by Rp-cAMPS. In human renal proximal tubule cells with *DRD1* gene silencing to eliminate the confounding effect of D₁R, fenoldopam still decreased mito-ROS production. By contrast, Sch23390, a D₁R and D₅R antagonist, increased mito-ROS production in the absence of D₁R, D₅R is constitutively active. The fenoldopam-mediated inhibition of mito-ROS production may have been related to autophagy because fenoldopam increased the expression of the autophagy hallmark proteins, autophagy protein 5 (ATG5), and the microtubule-associated protein 1 light chain (LC)3-II. In the presence of chloroquine or spautin-1, inhibitors of autophagy, fenoldopam further increased ATG5 and LC3-II expression, indicating an important role of D₅R in the positive regulation of autophagy. However, when autophagy was inhibited, fenoldopam was unable to inhibit ROS production. Indeed, the levels of these autophagy hallmark proteins were decreased in the kidney cortices of *Drd5*^{-/-} mice. Moreover, ROS production was increased in mitochondria isolated from the kidney cortices of *Drd5*^{-/-} mice, relative to *Drd5*^{+/+} littermates. In conclusion, D₅R-mediated activation of autophagy plays a role in the D₅R-mediated inhibition of mito-ROS production in the kidneys.

Keywords

Autophagy; Dopamine D₅ receptor; Hypertension; Mitochondria; Reactive oxygen species

Introduction

Reactive oxygen species (ROS) are a family of chemically derived reactive molecules from oxygen [1–3]. In addition to their established role in killing invading microorganisms, ROS, via direct oxidative damage or activation of cellular signaling pathways, are implicated in the pathogenesis of a wide variety of disorders, including hypertension [1–3]. There are many sources of ROS, e.g., NADPH oxidase [1–3], and mitochondria-derived ROS (mito-ROS) play an important role in the pathophysiology of hypertension [1–4].

Dopamine, produced in the kidney and via activation of dopamine receptors, regulates sodium balance and blood pressure [5–7]. Dopamine receptors are classified into D₁-like (D₁R and D₅R) receptors that stimulate adenylyl cyclases and D₂-like (D₂R, D₃R, and D₄R) receptors that inhibit adenylyl cyclases [5–7]. Abnormalities in renal dopamine production and D₁-like and D₂-like receptors are associated with hypertension and/or salt sensitivity in several ethnic groups [5–7]. The loci of human D₅R (4p15.1–16.1) and its pseudogenes (1q21.1 and 2p11.1–p11.2) are linked to human hypertension [8, 9]. Germline deletion of the *Drd5* gene (*Drd5*^{-/-}) in mice causes hypertension [10]. However, the mechanisms responsible for the increased blood pressure in *Drd5*^{-/-} mice are not completely understood.

In addition to genetic factors, many cellular factors, including ROS, are involved in the pathogenesis and maintenance of hypertension [1–4]. We have reported that ROS production in the kidneys and brain is greater in *Drd5*^{-/-} mice than in their *Drd5*^{+/+} littermates and that D₅R exerts its anti-oxidant properties in part by inhibiting NADPH oxidase activity [10]. NADPH oxidase is an important source of ROS production in renal tubule cells [1–3, 10–12], and the results of experiments inhibiting this enzyme complex with specific or nonspecific inhibitors support its importance in the regulation of blood pressure [1–3, 12, 13]. Recently, mitochondria-generated ROS have been reported to contribute to oxidative stress-mediated hypertension [1–4], but the mechanism is not known.

There is accumulating evidence linking autophagy and hypertension in response to oxidative stress [14]. Autophagy, an intracellular self-degradative process that delivers cytoplasmic constituents to lysosomes, has long been considered a cellular physiological process involved in the turnover of subcellular organelles and proteins [15, 16]. However, recent studies have indicated that autophagy plays important roles in the pathogenesis of human diseases, including those caused by oxidative stress [17]. Furthermore, autophagy can mediate inflammatory responses that induce oxidative stress [18, 19]. Oxidative stress increases the activity of both autophagosomes and auto-lysosomes; inhibition of autophagy attenuates autophagic flux [14], but autophagy protects against oxidative injury [20]. Moreover, autophagy is important in the removal of damaged mitochondria and polyubiquitinated proteins and in protection from damage caused by oxidative stress [14, 17]. D₅R can regulate the expression and activity of proteins that increase oxidative stress, for example, by triggering the ubiquitination and subsequent degradation of angiotensin II (Ang II) type 1 receptor (AT₁R) [10, 21–23]. However, investigations linking D₅R to autophagy and mitochondrial oxidative stress are sparse.

We investigated the potential role(s) of D₅R in mito-ROS production by determining whether the D₅R-mediated inhibition of renal cellular ROS production is caused in part by a decrease in mito-ROS production through an increase in autophagy.

Methods

Reagents

MitoTracker Green, MitoSOX Red (Mito-HE), and Amplex Red were purchased from Molecular Probes (Eugene, OR), and anti-autophagy protein 5 (ATG5) (Cat. No. 12994) and anti-LC3-II (Cat. No. 3868) antibodies were purchased from Cell Signaling Technology (Danvers, MA). The origins of the anti-D₁R and anti-D₅R antibodies in renal proximal tubule (RPT) cells and rat kidneys have been reported previously, and the antibodies have been verified in *D₁R*^{-/-} and *D₅R*^{-/-} mice [24–28]. Anti-Bax and anti-Bcl-xL antibodies were purchased from Santa Cruz Biotechnology (Santa Cruz, CA); anti-Mn-SOD and anti-Cu/Zn-SOD antibodies were purchased from Abcam (Cambridge, MA); an anti-prohibitin antibody was purchased from GeneTex (Irvine, CA); and anti-calnexin, anti-histone B4, and anti-GM130 antibodies were purchased from BD Transduction Laboratories (Lexington, KY). Culture media, fetal bovine serum (FBS), glutamine, and Lipofectamine transfection reagent were purchased from Invitrogen (Gaithersburg, MD). Percoll was purchased from GE Healthcare (Piscataway, NJ). NADPH was purchased from MP Biomedicals (Solon,

OH). An adenosine triphosphate (ATP) bioluminescence assay kit was purchased from Roche Applied Science (Indianapolis, IN). Spautin-1 was purchased from Griffin Biotech (Hong Kong, China). Fenoldopam, Sch23390, Rp-cAMPS, Sp-cAMPS, chloroquine, antimycin A, and other reagents were purchased from Sigma (St. Louis, MO).

Cell culture, siRNA, and transfection

Human embryonic kidney 293 (HEK293) cells expressing D₅R (D₅R-HEK293) and human RPT cells were cultured as previously described [23, 25]. Empty vector (EV)-transfected HEK293 and D₅R expression vector-transfected HEK293 cells (D₅R-HEK293 cells) were maintained in culture with 10 µg/mL blasticidin. The stable protein expression of D₅R in D₅R-HEK293 cells was confirmed before the actual experiments were performed (Supplementary Fig. 1). The RPT origins of human RPT cells were verified by staining with antibodies against γ -glutamyl transpeptidase, as previously described [25]. The cells were cultured in a 1:1 mixture of DMEM and Ham's F-12 medium supplemented with 5% FBS, selenium (5 ng/mL), insulin (5 µg/mL), transferrin (5 µg/mL), hydrocortisone (36 ng/mL), triiodothyronine (4 pg/mL), and epidermal growth factor (10 ng/mL).

Specific *DRD1*, *DRD5* (Santa Cruz Biotechnology), *ATG5*, and *LC3-II* (Cell Signaling Technology) siRNAs and their control siRNA constructs were transfected into human RPT cells or D₅R-HEK293 cells using Lipofectamine 2000 transfection reagent (Invitrogen) according to the manufacturer's instructions and our published procedure [29].

NADPH oxidase activity

NADPH oxidase activity was measured as previously described [10]. Equal amounts of cell membranes were incubated with lucigenin (5 µmol/L) for 10 min at 37 °C in a final volume of 1 mL of assay buffer. Recording of the dynamic chemiluminescence traces was started upon injection of NADPH (final concentration: 100 µmol/L) and continued for 180 s (Autolumet Plus LB953, EG&G Berthold, Bad Wildbad, Germany). The activity levels are expressed as arbitrary light units (ALUs) and were corrected for the protein concentration and duration of the experiment (ALU/s/mg protein).

Superoxide anion production

Superoxide anion production was measured using a cytochrome c assay, as previously described [10]. Cell homogenates in Hank's balanced salt solution (final concentration 1 mg/mL) were distributed in 96-well plates (final volume 200 µL/well). Cytochrome c (500 µmol/L) was added, and the homogenates were incubated in the presence or absence of superoxide dismutase (SOD, 200 U/mL) at room temperature for 30 min. Cytochrome c reduction was measured by reading the absorbance at 550 nm on a microplate reader.

Confocal fluorescence microscopy

Confocal fluorescence microscopy was performed as previously described [29, 30]. The mito-ROS signals in live cells stained with MitoSOX Red were monitored by laser scanning confocal microscopy (LSM 510, Carl Zeiss). The cells were treated with vehicle or the D₁-like receptor agonist fenoldopam (1 µM, 15 min) in the presence or absence of the D₁-like receptor antagonist Sch23390 (1 µM, 45 min). After washing the cells with

Hank's balanced salt solution, the cells were incubated with 5 μ M MitoSOX Red for 10 min. Images were captured with excitation at 405 nm and emission at 590 nm under a Plan-Apochromat 63 \times /1.4 Oil NA objective. The MitoSOX Red fluorescence density was semiquantified in 3–5 random fields from 25–40 cells [30]. MitoTracker Green was used to identify mitochondria. Endogenous light chain (LC)3-II was immunostained with an anti-LC3-II antibody (Cell Signaling Technology). The fluorescence intensity was estimated from the range within the initial linear phase to minimize potential problems arising from mitochondrial dye saturation and leakage.

Western blotting

Western blotting was performed as previously described [10, 25]. Samples (D₅R-HEK293, human RPT cells, kidney cortices, and isolated mitochondria) were adjusted to the same protein concentration. The proteins were separated by sodium dodecyl sulfate-polyacrylamide gel electrophoresis, transferred onto a nitrocellulose membrane, and then probed with primary antibodies and appropriate horseradish peroxidase-conjugated secondary antibodies. The images were visualized by chemiluminescence.

ATP assay

ATP concentrations were quantified as previously described [30, 31]. In brief, human RPT cells were grown in 25-cm tissue culture dishes. After harvesting the cells by centrifugation, the cell pellets were sonicated in 800 μ L of lysis buffer. The ATP released in 300 μ L of buffer (100 mM Tris-Cl, pH 7.75; 4 mM EDTA) was boiled for 2 min. ATP bioluminescence was monitored by a microplate lumen-ometer (Centro LB 960, Berthold Technologies, Bad Wildbad, Germany).

Generation of *Drd5*^{-/-} mice

The method used for generation of *Drd5*^{-/-} mice has been reported [10, 23]. F6 generation *Drd5*^{-/-} mice on a C57Bl/6 (>98% congenic) background and their sex-matched wild-type littermates were used in this study. Fenoldopam (1 mg/kg body weight, 0.5 mL) or vehicle (saline, for control) was injected intraperitoneally daily for 7 days. Subsequently, the kidneys were collected, and their cortices were excised and homogenized for immunoblotting of autophagy marker proteins. Mitochondria were isolated and purified for H₂O₂ production assays.

The animal protocols were reviewed and approved by the Georgetown University, Children's National Medical Center, and University of Maryland School of Medicine Animal Care and Use Committees.

Mitochondria isolation and H₂O₂ measurement

Mitochondria were isolated from D₅R-HEK293 cells, human RPT cells, and mouse kidney cortices by Percoll density gradient centrifugation as previously described [32] with modifications. In brief, cell pellets or minced kidney cortices were homogenized. The homogenates were suspended in a buffer (pH 7.4) containing 225 mM mannitol, 75 mM sucrose, 5 mM HEPES, 1 mM ethylene glycol-bis (2-aminoethylether)-*N,N,N',N'*-tetraacetic acid (EGTA), and 1 mg/mL fatty acid-free bovine serum albumin and centrifuged

at $1300 \times g$ for 3 min. The pelleted material was resuspended in the above buffer and centrifuged at $1300 \times g$ for 3 min. The combined supernatants were then centrifuged at $21,000 \times g$ for 10 min. The pellets were suspended in 15% Percoll and gently transferred onto the surface of 23% Percoll without touching the 40% Percoll. The gradients were centrifuged at $29,000 \times g$ for 8 min. The mitochondria were isolated from the interface of the 23 and 40% Percoll. The isolated mitochondria, which had no measurable NADPH oxidase activity and were characterized with pyruvate/malate (5 mM) and succinate (4 mM) in a medium containing 125 mM KCl, 2 mM K_2HPO_4 , 3 mM HEPES, 4 mM $MgCl_2$, 3 mM ATP, and 0.2% fatty acid-free bovine serum albumin (pH 7.2), showed coupling of oxidative phosphorylation and normal respiration. The purity of the mitochondrial fraction was confirmed by immunoblotting markers of organelles.

Mito-ROS production by isolated mitochondria was measured with Amplex Red in the presence of exogenous superoxide dismutase (40 U/mL) and horseradish peroxidase (10 U/mL), as described previously [33] with modifications. The fluorescence intensity was measured with a microplate reader in 96-well plates at an excitation wavelength of 530 nm and an emission wavelength of 590 nm. The rate of H_2O_2 production was linear for a fluorescence density up to $3 \mu\text{mol/L}$ in the standard curve. ROS production is expressed in picomoles of H_2O_2 per mg of mitochondrial protein/min.

Statistical analysis

The results are expressed as the mean \pm standard deviation, as indicated. Significant differences among groups ($n > 2$) were determined by one-way factorial ANOVA and the Newman–Keuls test, and significant differences between two groups were determined by Student's *t* test. $P < 0.05$ was considered to indicate statistical significance (SigmaStat 3.0, SPSS Inc, Chicago, IL).

Results

Activation of D₅R decreased ROS production in mitochondria from D₅R-HEK293 cells

Consistent with our previous report [10], stimulation of D₅R with fenoldopam decreased both cellular superoxide ($O_2^{\cdot-}$) production ($0.296 \pm 0.033 \text{ OD}_{550}/\text{min}/\text{mg}$ vs vehicle $0.493 \pm 0.024 \text{ OD}_{550}/\text{min}/\text{mg}$, $P < 0.05$), as quantified by cytochrome *c* reduction (Supplementary Fig. 2A), and NADPH oxidase activity ($2183 \pm 123 \text{ ALU}/\text{min}/\text{mg}$ vs vehicle $2449 \pm 52 \text{ ALU}/\text{min}/\text{mg}$, $P < 0.01$), as quantified by lucigenin assay (Supplementary Fig. 2B), in D₅R-HEK293 cells. However, $O_2^{\cdot-}$ production was lower in the presence of both fenoldopam and apocynin ($10 \mu\text{M}$), an NADPH oxidase inhibitor, than in the presence of apocynin alone ($0.187 \pm 0.012 \text{ OD}_{550}/\text{min}/\text{mg}$ vs apocynin alone $0.358 \pm 0.045 \text{ OD}_{550}/\text{min}/\text{mg}$, $P < 0.01$) (Supplementary Fig. 2A). By contrast, under the same experimental conditions, fenoldopam did not enhance the apocynin-mediated inhibition of NADPH oxidase activity ($1890 \pm 147 \text{ ALU}/\text{min}/\text{mg}$ vs apocynin alone $1906 \pm 77 \text{ ALU}/\text{min}/\text{mg}$, $P > 0.05$) (Supplementary Fig. 2B). These results indicate that fenoldopam decreased ROS production by an additional mechanism or mechanisms other than inhibition of NADPH oxidase activity.

Because mitochondria are important sources of cellular ROS production in the kidneys [1, 3, 4], we next determined whether mitochondria are the additional sources of ROS targeted by D₅R, as observed in Supplementary Fig. 2A. Mitochondria isolated from D₅R-HEK293 cells (Fig. 1A) produced less hydrogen peroxide (H₂O₂) than those from EV-transfected HEK293 cells (Fig. 1B). Fenoldopam treatment further decreased H₂O₂ production in D₅R-HEK293 cells but had no effect on EV-transfected HEK293 cells (Fig. 1B). In intact D₅R-HEK293 cells, fenoldopam decreased mito-ROS production, as detected with MitoSOX Red, a hydroethidine (HE)-derived fluorescent dye (Fig. 1C). The colocalization of MitoSOX Red staining with MitoTracker Green staining indicated the mitochondrial origin of the generated ROS (Fig. 1C). The inhibitory effect of fenoldopam on ROS production was prevented by Sch23390, a D₁-like receptor antagonist, in both isolated mitochondria (Fig. 1B) and intact cells (Fig. 1C, D). These findings indicate that fenoldopam, a D₁R/D₅R agonist, decreased ROS production by stimulating D₅R (D₁R is not expressed in D₅R-HEK293 cells). Sch23390, a D₁R/D₅R antagonist but a D₅R antagonist in the absence of D₁R, itself increased ROS production (Fig. 1B–D), which could be due to its blockade of D₅R's constitutive activity [10] because, as stated earlier, HEK293 cells do not express D₁R. H₂O₂ production was increased by antimycin A, a Qi site inhibitor of mitochondrial electron transport chain (ETC) Complex III and prevented the inhibitory effect of fenoldopam (Fig. 1B). By contrast, rotenone, a Complex I inhibitor (Supplementary Fig. 3), had no effect on the inhibitory effect of fenoldopam, indicating that Complex III, not Complex I, is the target of the D₅R-mediated decrease in mito-ROS production. H₂O₂ production, as expected, was decreased by catalase despite the presence of antimycin A (Fig. 1B).

Activation of D₅R, similar to activation of D₁R, stimulates cAMP and protein kinase A (PKA) [5–7]. To determine whether the D₅R-mediated inhibition of mito-ROS is cAMP-dependent, D₅R-HEK293 cells were pretreated with Rp-cAMPS (Fig. 2), a selective inhibitor of PKA [34]. Rp-cAMPS alone did not affect H₂O₂ production but prevented the inhibitory effect of fenoldopam. Sch23390 itself increased H₂O₂ production; as indicated above, this effect was probably mediated by inhibition of the constitutive activity of D₅R [10]. This stimulatory effect of Sch23390 was also inhibited by Rp-cAMPS. Sp-cAMPS, a PKA activator, decreased mito-ROS production (Fig. 2), an effect that was prevented by Rp-cAMPS, indicating the specificity of the effect of Sp-cAMPS on the cAMP pathway. All these results indicate that the D₅R-mediated inhibition of mito-ROS production is cAMP-dependent.

Activation of D₅R decreased ROS production in mitochondria from human RPT cells

To study further the effect of D₅R on mito-ROS production in connection with its potential role in regulating renal sodium transport and ultimately blood pressure [10, 23], we studied mito-ROS production in human RPT cells [21]. Similar to the observations in D₅R-HEK293 cells (Fig. 1), fenoldopam decreased mito-ROS production in human RPT cells. This effect was inhibited by Sch23390, a D₁R/D₅R antagonist, which increased mito-ROS production when used alone (Fig. 3A).

Since no commercially available antagonist or agonist can distinguish the effect of D₅R from that of D₁R, both of which are expressed endogenously in human RPT cells, we

silenced the expression of D₁R or D₅R by transfection with either *DRD1*- or *DRD5*-specific siRNA (Supplementary Fig. 4). With *DRD1* silencing, fenoldopam still decreased mito-ROS production in both isolated mitochondria (Fig. 3B) and intact human RPT cells (Fig. 3C). There was no effect of fenoldopam when *DRD5* was silenced, indicating that D₅R, not D₁R, inhibits ROS production in the mitochondria. Similar to the D₅R-HEK293 results, the inhibitory effect of fenoldopam on ROS production was reversed by the D₁-like receptor antagonist Sch23390 in human RPT cells with intact D₁R (Fig. 3A) or silenced D₁R (Fig. 3B), affirming that the effect of fenoldopam is exerted via D₅R.

Similar to the findings in D₅R-HEK293 cells (Fig. 1), Sch23390 alone increased mito-ROS production in D₁R-intact (Fig. 3A) and D₁R-silenced (Fig. 3B) human RPT cells. *DRD5* silencing alone also increased H₂O₂ production (Fig. 3B), similar to the situation observed with Sch23390 in D₅R-HEK293 cells (Fig. 2). These results support the notion that D₅R is constitutively active [10]. By contrast, fenoldopam failed to decrease and Sch23390 failed to increase mito-ROS production in human RPT cells with silenced *DRD5* (Fig. 3B), indicating a minimal role of D₁R in the regulation of mito-ROS in human RPT cells.

Activation of D₅R inhibited mito-ROS through an increase in autophagy

Recent evidence suggests that oxidative stress regulates autophagy [14, 16, 17] and that products of dopamine oxidation stimulate autophagy in a neuroblastoma cell line [35]. Therefore, we investigated whether D₅R stimulation regulates autophagy. The D₁-like receptor agonist fenoldopam inhibited ROS production (Figs. 1–3) [10]. In D₅R-HEK293 cells, fenoldopam increased cellular autophagy, as shown by the increase in LC3-II immunostaining (Supplementary Fig. 5). Consistently, fenoldopam also increased the protein expression of ATG5 and LC3-II (Fig. 4A), both of which are involved in autophagy. In the presence of chloroquine, an inhibitor of autophagosome-lysosome fusion and subsequently lysosome-mediated proteolysis [36], the ATG5 and LC3-II protein expression levels were increased further by fenoldopam. These results indicate that the fenoldopam-induced increases in the expression of ATG5 and LC3-II protein were due to an increase in autophagic flux rather than to blockade of the degradation of these proteins. Consistent with this interpretation is the demonstration that Sch23390, an antagonist of D₅R (in the absence of D₁R), decreased the protein expression of ATG5 and LC3-II by blocking D₅R activation. This effect was blocked by chloroquine (Fig. 4B), probably because chloroquine prevented the degradation of ATG5 and LC3-II protein [36].

In *DRD1*-silenced human RPT cells, fenoldopam also increased the protein expression of ATG5 and LC3-II (Fig. 5A) but not the expression of the proapoptotic protein Bax or the antiapoptotic protein Bcl-xL (Fig. 5B). These results were associated with decreases in cellular ATP concentrations (Fig. 5C), indicating that D₅R activation increased autophagy but not apoptosis, which is related to a decrease in mitochondrial energy production in human RPT cells. We then studied whether autophagy involves D₅R-mediated inhibition of mito-ROS production using chloroquine. Chloroquine alone slightly but significantly increased mito-ROS production in D₁R-silenced human RPT cells but did not affect mito-ROS production in D₅R-silenced human RPT cells (Fig. 5D). Similar results were observed with spautin-1, another autophagy inhibitor (Supplementary Fig. 6). Indeed, when

autophagy was inhibited by either chloroquine (Fig. 5E) or spautin-1 (Supplementary Fig. 6), fenoldopam was unable to decrease mito-ROS in human RPT cells with intact D₅R when *DRD1* was silenced. These results indicate that stimulation of autophagy is involved in the D₅R-mediated decrease in mito-ROS production in human RPT cells. Moreover, in the presence of apocynin, an NADPH oxidase inhibitor, fenoldopam was still able to decrease mito-ROS production in *DRD5*-intact and *DRD1*-silenced (Fig. 5E) human RPT cells, confirming the involvement of a non-NADPH oxidase-mediated mechanism, presumably related to mito-ROS, similar to that observed in D₅R-HEK293 cells (Supplementary Fig. 2A).

Autophagy protein expression and mito-ROS production in *Drd5*^{-/-} mouse kidneys

The protein expression levels of ATG5 and LC3-II in *Drd5*^{-/-} mouse kidney cortices were lower than those in kidney cortices obtained from wild-type *Drd5*^{+/+} littermates (Fig. 6A), indicating that the kidney cortices of *Drd5*^{-/-} mice have decreased autophagy. Mitochondria from the kidney cortices of these mice were isolated (Supplementary Fig. 7) for determination of H₂O₂ production. As shown in Fig. 6B, H₂O₂ production in mitochondria isolated from the kidney cortices of *Drd5*^{-/-} mice was significantly higher than in mitochondria isolated from the kidney cortices of *Drd5*^{+/+} mice.

Treatment of *Drd5*^{+/+} mice with fenoldopam significantly decreased mitochondrial H₂O₂ production (Fig. 6B) and increased ATG5 and LC3-II protein expression in kidney cortices (Supplementary Fig. 8A). By contrast, fenoldopam treatment of *Drd5*^{-/-} mice did not change H₂O₂ production by isolated renal mitochondria (Fig. 6B) or the protein expression of ATG5 and LC3-II (Supplementary Fig. 8B). These findings indicated that the fenoldopam-mediated increase in autophagy and decrease in mito-ROS were D₅R- but not D₁R-dependent in vivo, which corroborated the in vitro observations.

As expected, antimycin A increased H₂O₂ production in mitochondria isolated from kidney cortices from both *Drd5*^{-/-} and *Drd5*^{+/+} mice, and catalase prevented the stimulatory effect of antimycin A in both *Drd5*^{-/-} and *Drd5*^{+/+} mice (Fig. 6B), consistent with the results of *DRD5* silencing studies in human RPT cells (Fig. 5D). Neither Mn-SOD nor Cu/Zn-SOD protein expression in kidney cortices differed between *Drd5*^{-/-} and *Drd5*^{+/+} mice (Fig. 6C).

Discussion

Oxidative stress is implicated in many pathological conditions, such as hypertension, atherosclerosis, and chronic kidney diseases [1–5, 10, 12–14, 19, 20, 37]. Mitochondria generate more than half of cellular ROS in the basal state [4]. Dopamine, through D₁-like (D₁R and D₅R) and D₂-like (D₂R, D₃R and D₄R) receptors, decreases ROS production in RPT cells and kidneys from humans and animals [1, 5–7, 10, 21, 23]. D₅R negatively regulates ROS production, in part through inhibition of NADPH oxidase expression and activity [10]. The current study demonstrates that fenoldopam, a D₅R agonist (in the absence of D₁R), decreases mito-ROS production in D₅R-HEK293 and human RPT cells and the kidneys of *Drd5*^{+/+} mice but not in EV-HEK293 cells lacking D₅R, *DRD5*-silenced human RPT cells, or the kidneys of *Drd5*^{-/-} mice.

Mitochondria have long been recognized as a major source of ROS in most eukaryotic cells [4]. However, the roles of mitochondrial dysfunction in the pathogenesis of cardiovascular disorders [38] and the importance of mito-ROS in the pathogenesis of hypertension are not as well appreciated as the roles of ROS produced by NADPH oxidase, partly due to the difficulty in accurately measuring mito-ROS production [37, 39–41]. Cytochrome *c* reduction assays, high-performance liquid chromatography, electron paramagnetic resonance spectroscopy, nitroblue tetrazolium assays, chemiluminescence-based assays, and immunospin trapping have all been used to detect cellular or extracellular superoxide [39–41]. However, due to cumbersome sample preparation methods, low sensitivity, or the need for expensive instruments, these available techniques are not widely used for measurement of mito-ROS in living cells [39–41]. Fluorescence microscopy with a fluorescence-based probe targeting mitochondria enables sensitive, real-time monitoring of mito-ROS signals in individual live cells. Mito-HE, a derivative of HE with a hexyl linker to triphenylphosphonium that accumulates preferentially in mitochondria by several hundred fold [42, 43], was used to monitor mito-ROS production in intact cells. Fluorescent 2-hydroxyethidium, which is generated by the reaction of Mito-HE with ROS, is a relatively reliable indicator of mito-ROS signaling in a biological context [43]. Using Mito-HE (which is also known as MitoSOX Red) as the probe for ROS, we found that activation of D₅R attenuated mitochondrial oxidative stress in live D₅R-HEK293 and human RPT cells. To avoid the potential technical limitations of Mito-HE [42] and cross-talk with NADPH oxidase-derived ROS in intact cells, additional experiments were performed in mitochondria isolated from D₅R-HEK293 and human RPT cells in which the other D₁-like receptor, D₁R, was silenced and in kidney cortices of *Drd5*^{-/-} and *Drd5*^{+/+} mice. All results of these studies consistently show that D₅R, in the absence of D₁R, negatively regulates mito-ROS production.

The production of ROS by mitochondria is caused by leakage of electrons from the ETC, with Complex I and Complex III conventionally recognized as the major sites [44, 45]. In vitro studies have demonstrated that Complex I is the major site for ROS production when cells do not produce ATP with high NADH/NAD⁺ and CoQH₂/CoQ ratios and high proton motive force [44]. However, under most conditions, mitochondria in cells synthesize ATP. In this situation, Complex III and other sites are important sites for ROS production in mitochondria [44, 45]. Our in vitro data demonstrated that ROS production was significantly increased upon inhibition of the Complex III Qi site with antimycin A but not upon inhibition of Complex I with rotenone. Moreover, antimycin A, but not rotenone, prevented the inhibitory effect of fenoldopam on ROS production in intact D₅R-HEK cells, indicating that D₅R may directly or indirectly interact with Complex III rather than Complex I. The site(s) of ROS production within the mitochondria depend(s) on the cell bioenergetic status and the substrate being oxidized [44–46]. Whether D₅R targets Complex III in vivo under different bioenergetic conditions or mechanisms requires further investigation.

Mitochondria and NADPH oxidases are the two main sources of cellular ROS, and it is believed there is a vicious cycle between these two sources of ROS; NADPH oxidase-derived ROS increase mito-ROS formation, and mito-ROS activate NADPH oxidase [47]. We have reported that D₁-like receptor activation decreases renal ROS production in part through inhibition of NADPH oxidase in the kidneys [10, 48]. Yang et al. have also reported

that D₁-like receptors decrease NADPH oxidase-mediated ROS production in human RPT cells [49]. However, D₅R, not D₁R, decreases ROS production, in part by increasing paraoxonase 2 protein levels [49]. Our present study demonstrates that D₅R, not D₁R, decreases Mito-ROS production, which is consistent with a recent report that paraoxonase 2 decreases mitochondrial ROS production in cardiomyocytes [50]. The decrease in mito-ROS production mediated by the D₁R/D₅R agonist fenoldopam was not abrogated by the presence of the NADPH oxidase inhibitor apocynin in human RPT cells deficient in D₁R but with intact D₅R. This result indicates that the D₅R-mediated decrease in mito-ROS production is not downstream of its inhibition of NADPH oxidase activity.

Dopamine increases LC3-II expression and autophagy in neuroblastoma cells [35]. D₃R induces autophagy under hyperammonia [51]. By contrast, inhibition of D₂R activity induces autophagy in neuroblastoma cells [52] and cardiomyocytes [53]. However, inhibition of D₄R activity also disrupts autophagosome-lysosomal fusion [54]. In our study, we demonstrated that activation of D₅R using fenoldopam at concentrations that inhibit ROS production [10] increased autophagic protein expression and activation in human RPT cells, which was confirmed in the kidneys of *Drd5*^{+/+} mice, indicating that D₅R, like D₃R and D₄R, is involved in the regulation of autophagy. Of note, all dopamine receptors are expressed in the kidneys, and their expression is different at different stages of development [25–27, 55–57]. Thus, it is possible that the role of D₅R in autophagy could be different from that of other dopamine receptors in different nephron segments at different stages of development.

Autophagy can be both a cause and consequence of oxidative stress [14, 17]. Mitochondria are both the major sources and targets of ROS; therefore, mitochondria could play critical roles in the cellular responses to oxidative stress. On the one hand, mito-ROS, via multiple signaling pathways, can lead to downregulation or upregulation of autophagy [14, 17, 58]. On the other hand, autophagy regulates ROS signaling or cellular consequences in response to oxidative stress [14]. Autophagic deficiency in mouse embryonic fibroblasts protects against H₂O₂-induced cell death [59]. However, hepatocyte-specific deletion of *Atg5* in mice induces oxidative stress in these cells [60]; pancreas-specific disruption of *Atg5* in mice also increases ROS production in this organ [61]. Intestinal epithelial cell-specific deletion of *Atg5* in mice decreases the basal intestinal epithelial cell mitochondrial membrane potential and increases ROS production [62], suggesting that deficiency of autophagy could lead to an increase in ROS production that may be related to mitochondrial dysfunction.

Mild oxidative stress induces autophagy, while severe oxidative stress inhibits autophagy [17, 58], and high concentrations of dopamine increase autophagy via oxidative products of dopamine [35]. High, cytotoxic concentrations of dopamine (>100 μM) increase oxidative stress, but low, noncytotoxic concentrations of dopamine decrease oxidative stress [63, 64]. Stimulation of D₁-like receptors by the D₁-like receptor agonist fenoldopam decreases ROS production [10], but the effect of fenoldopam on autophagy has not been reported. Ang II promotes autophagy, which is mediated by mito-ROS in podocytes [65, 66]. D₅R activation promotes the ubiquitination and proteasomal degradation of AT₁R [21–23], and germline deletion of *Drd5* in mice increases renal AT₁R expression [23]. By contrast, AT₁R blockade with losartan or germline deletion of *Agtr1* in mice increases D₅R protein expression

[7, 67]. Therefore, treatment with an AT₁R blocker should increase the inhibitory effect of fenoldopam on mito-ROS production but negate the stimulatory effect of fenoldopam on autophagy. However, fenoldopam decreases ROS production and stimulates autophagy, indicating that the effect of fenoldopam on autophagy is direct (vide infra) and not mediated through ROS. It is also known that enhancement of ubiquitination or inhibition of the proteasome pathway plays an important role in the induction of autophagy associated with mitochondrial oxidative stress [68–70]. However, D₅R activates both the ubiquitination and proteasome pathways in addition to inhibiting ROS production, as described previously [23]. Studies by others have shown that the increase in autophagy caused by ROS is mediated by AMPK [71], which can be stimulated by cAMP [71, 72], the levels of which are increased by D₅R [5–7]. The presence of soluble adenylyl cyclase both outside and inside the mitochondria suggests that phosphorylation of mitochondrial proteins may be a major regulatory mechanism for mitochondrial function [73]. cAMP-PKA signaling can regulate all steps of autophagy [74]. Therefore, cAMP signaling could act as a bridge between D₅R in the cell membrane and mitochondria to regulate mitochondrial function. However, depending on the local microenvironments of tissues and cells, activation of cAMP signaling could induce [75, 76], reduce [77], or have no effect [78] on autophagy. Thus, while both D₁R and D₅R increase cAMP production and decrease ROS production [5–7, 10, 48], these two D₁-like receptors have different effects on autophagy and ROS production: D₅R, but not D₁R, stimulates autophagy and inhibits the production of ROS in mitochondria. D₁R increases adenylyl cyclase type 5/6 proteins in lipid rafts, while D₅R increases adenylyl cyclase type 5/6 proteins in nonlipid rafts [79]. We speculate that these differential effects of D₅R and D₁R could be due to their differential expression in lipid and nonlipid raft microenvironments, their coupling to different isoforms of adenylyl cyclases [79], or other unknown factors; these possibilities warrant further study. Nevertheless, our current study shows that D₅R-mediated decreases in ROS production are probably due to increases in cAMP production and subsequent induction of autophagy.

In summary, activation of D₅R, independent of D₁R decreased mito-ROS production in D₅R-HEK293 and RPT cells. This effect was mimicked by the PKA activator Sp-cAMPS and was attenuated by the PKA inhibitor Rp-cAMPS and the autophagy inhibitors chloroquine and spautin-1. ROS production was increased in mitochondria isolated from the kidney cortices of *Drd5*^{-/-} mice relative to their wild-type littermates. Furthermore, the renal protein expression of autophagy hallmark proteins was increased by fenoldopam, a D₅R agonist (in the absence of D₁R), in vitro and in vivo. These results suggest that D₅R negatively regulates ROS production in a cAMP- and autophagy-dependent manner.

Supplementary Material

Refer to Web version on PubMed Central for supplementary material.

Acknowledgements

This study was supported in part by grants from the National Institutes of Health (HL074940, HL023081, DK039308, HL092196, DK119652, and DK090918), the Children's National Medical Center Intramural Avery Award, the National Natural Science Foundation of China (81670698, 91739119, 81670406, 30971186), the Second Hospital of Dalian Medical University Start-up Funds, and the Department of Education of Liaoning Province Grant (L2016020).

References

1. Araujo M, Wilcox CS. Oxidative stress in hypertension: role of the kidney. *Antioxid Redox Signal*. 2014;20:74–101. [PubMed: 23472618]
2. Loperena R, Harrison DG. Oxidative stress and hypertensive diseases. *Med Clin North Am*. 2017;101:169–93. [PubMed: 27884227]
3. Montezano AC, Dulak-Lis M, Tsiropoulou S, Harvey A, Briones AM, Touyz RM. Oxidative stress and human hypertension: vascular mechanisms, biomarkers, and novel therapies. *Can J Cardiol*. 2015;31:631–41. [PubMed: 25936489]
4. Addabbo F, Montagnani M, Goligorsky MS. Mitochondria and reactive oxygen species. *Hypertension*. 2009;53:885–92. [PubMed: 19398655]
5. Zhang MZ, Harris RC. Antihypertensive mechanisms of intra-renal dopamine. *Curr Opin Nephrol Hypertens*. 2015;24:117–22. [PubMed: 25594544]
6. Asghar M, Tayebati SK, Lokhandwala MF, Hussain T. Potential dopamine-1 receptor stimulation in hypertension management. *Curr Hypertens Rep*. 2011;13:294–302. [PubMed: 21633929]
7. Zeng C, Jose PA. Dopamine receptors: important antihypertensive counterbalance against hypertensive factors. *Hypertension*. 2011; 57:11–7. [PubMed: 21098313]
8. Allayee H, de Bruin TW, Michelle Dominguez K, Cheng LS, Ipp E, Cantor RM, et al. Genome scan for blood pressure in Dutch dyslipidemic families reveals linkage to a locus on chromosome 4p. *Hypertension*. 2001;38:773–8. [PubMed: 11641285]
9. Cohn DH, Shohat T, Yahav M, Ilan T, Rechavi G, King L, et al. A locus for an autosomal dominant form of progressive renal failure and hypertension at chromosome 1q21. *Am J Hum Genet*. 2000; 67:647–51. [PubMed: 10930359]
10. Yang Z, Asico LD, Yu P, Wang Z, Jones JE, Escano CS, et al. D5 dopamine receptor regulation of reactive oxygen species production, NADPH oxidase, and blood pressure. *Am J Physiol Regul Integr Comp Physiol*. 2006;290:R96–104. [PubMed: 16352863]
11. Saez F, Hong NJ, Garvin JL. Luminal flow induces NADPH oxidase 4 translocation to the nuclei of thick ascending limbs. *Physiol Rep*. 2016;4:e12724. [PubMed: 27033446]
12. Yang Q, Wu FR, Wang JN, Gao L, Jiang L, Li HD, et al. Nox4 in renal diseases: an update. *Free Radic Biol Med*. 2018;124:466–72. [PubMed: 29969717]
13. Haque MZ, Majid DS. Reduced renal responses to nitric oxide synthase inhibition in mice lacking the gene for gp91phox subunit of NAD(P)H oxidase. *Am J Physiol Ren Physiol*. 2008;295: F758–64.
14. Ryter SW, Bhatia D, Choi ME. Autophagy: a lysosome-dependent process with implications in cellular redox homeostasis and human disease. *Antioxid Redox Signal*. 2019;30:138–59. [PubMed: 29463101]
15. Green DR, Levine B. To be or not to be? How selective autophagy and cell death govern cell fate. *Cell*. 2014;157:65–75. [PubMed: 24679527]
16. Dikic I, Elazar Z. Mechanism and medical implications of mammalian autophagy. *Nat Rev Mol Cell Biol*. 2018;19:349–64. [PubMed: 29618831]
17. Woodall BP, Gustafsson AB. Autophagy—a key pathway for cardiac health and longevity. *Acta Physiol*. 2018;20:e13074.
18. Sanderson RD, Elkin M, Rapraeger AC, Ilan N, Vlodaysky I. Heparanase regulation of cancer, autophagy and inflammation: new mechanisms and targets for therapy. *FEBS J*. 2017;284:42–55. [PubMed: 27758044]
19. Peña-Oyarzun D, Bravo-Sagua R, Diaz-Vega A, Aleman L, Chiong M, Garcia L, et al. Autophagy and oxidative stress in noncommunicable diseases: a matter of the inflammatory state. *Free Radic Biol Med*. 2018;124:61–78. [PubMed: 29859344]
20. Wible DJ, Bratton SB. Reciprocity in ROS and autophagic signaling. *Curr Opin Toxicol*. 2018;7:28–36. [PubMed: 29457143]
21. Gildea JJ, Wang X, Jose PA, Felder RA. Differential D1 and D5 receptor regulation and degradation of the angiotensin type 1 receptor. *Hypertension*. 2008;51:360–6. [PubMed: 18172057]

22. Jean-Charles PY, Snyder JC, Shenoy SK. Ubiquitination and deubiquitination of G protein-coupled receptors. *Prog Mol Biol Transl Sci.* 2016;141:1–55. [PubMed: 27378754]
23. Li H, Armando I, Yu P, Escano C, Mueller SC, Asico L, et al. Dopamine 5 receptor mediates Ang II type 1 receptor degradation via a ubiquitin-proteasome pathway in mice and human cells. *J Clin Investig.* 2008;118:2180–9. [PubMed: 18464932]
24. Hollon TR, Bek MJ, Lachowicz JE, Ariano MA, Mezey E, Ramachandran R, et al. Mice lacking D5 dopamine receptors have increased sympathetic tone and are hypertensive. *J Neurosci.* 2002;22:10801–10. [PubMed: 12486173]
25. Sanada H, Jose PA, Hazen-Martin D, Yu PY, Xu J, Bruns DE, et al. Dopamine-1 receptor coupling defect in renal proximal tubule cells in hypertension. *Hypertension.* 1999;33:1036–42. [PubMed: 10205244]
26. O'Connell DP, Botkin SJ, Ramos SI, Sibley DR, Ariano MA, Felder RA, et al. Localization of dopamine D1A receptor protein in rat kidneys. *Am J Physiol.* 1995;268:F1185–97. [PubMed: 7611459]
27. Ennis RC, Asico LD, Armando I, Yang J, Feranil JB, Jurgens JA, et al. Dopamine D₁-like receptors regulate the α_1 A-adrenergic receptor in human renal proximal tubule cells and D₁-like dopamine receptor knockout mice. *Am J Physiol Ren Physiol.* 2014;307:F1238–48.
28. Wang X, Li F, Jose PA, Ecelbarger CM. Reduction of renal dopamine receptor expression in obese Zucker rats: role of sex and angiotensin II. *Am J Physiol Ren Physiol.* 2010;299:F1164–70.
29. Li H, Li HF, Felder RA, Periasamy A, Jose PA. Actin cytoskeleton-dependent Rab GTPase-regulated angiotensin type I receptor lysosomal degradation studied by fluorescence lifetime imaging microscopy. *J Biomed Opt.* 2008;13:031206. [PubMed: 18601530]
30. Lee H, Abe Y, Lee I, Shrivastav S, Crusan AP, Huttemann M, et al. Increased mitochondrial activity in renal proximal tubule cells from young spontaneously hypertensive rats. *Kidney Int.* 2014;85:561–9. [PubMed: 24132210]
31. Lee I, Salomon AR, Ficarro S, Mathes I, Lottspeich F, Grossman LI, et al. cAMP-dependent tyrosine phosphorylation of subunit I inhibits cytochrome c oxidase activity. *J Biol Chem.* 2005;280: 6094–100. [PubMed: 15557277]
32. Polster BM, Nicholls DG, Ge SX, Roelofs BA. Use of potentiometric fluorophores in the measurement of mitochondrial reactive oxygen species. *Methods Enzymol.* 2014;547:225–50. [PubMed: 25416361]
33. Votyakova TV, Reynolds IJ. Detection of hydrogen peroxide with Amplex Red: interference by NADH and reduced glutathione auto-oxidation. *Arch Biochem Biophys.* 2004;431:138–44. [PubMed: 15464736]
34. Lochner A, Moolman JA. The many faces of H89: a review. *Cardiovasc Drug Rev.* 2006;24:261–74. [PubMed: 17214602]
35. Gimenez-Xavier P, Francisco R, Santidrian AF, Gil J, Ambrosio S. Effects of dopamine on LC3-II activation as a marker of autophagy in a neuroblastoma cell model. *Neurotoxicology.* 2009;30:658–65. [PubMed: 19410601]
36. Mauthe M, Orhon I, Rocchi C, Zhou X, Luhr M, Hijlkema KJ, et al. Chloroquine inhibits autophagic flux by decreasing autophagosome-lysosome fusion. *Autophagy.* 2018;14:1435–55. [PubMed: 29940786]
37. Kirkman DL, Muth BJ, Ramick MG, Townsend RR, Edwards DG. Role of mitochondria-derived reactive oxygen species in microvascular dysfunction in chronic kidney disease. *Am J Physiol Ren Physiol.* 2018;314:F423–9.
38. Bonora M, Wieckowski MR, Sinclair DA, Kroemer G, Pinton P, Galluzzi L. Targeting mitochondria for cardiovascular disorders: therapeutic potential and obstacles. *Nat Rev Cardiol.* 2019;16: 33–55. [PubMed: 30177752]
39. Griendling KK, Touyz RM, Zweier JL, Dikalov S, Chilian W, Chen YR, et al. Measurement of reactive oxygen species, reactive nitrogen species, and redox-dependent signaling in the cardiovascular system: a scientific statement from the American Heart Association. *Circ Res.* 2016;119:e39–75. [PubMed: 27418630]

40. Lee R, Margaritis M, Channon KM, Antoniades C. Evaluating oxidative stress in human cardiovascular disease: methodological aspects and considerations. *Curr Med Chem*. 2012;19:2504–20. [PubMed: 22489713]
41. Mason RP. Imaging free radicals in organelles, cells, tissue, and in vivo with immuno-spin trapping. *Redox Biol*. 2016;8:422–9. [PubMed: 27203617]
42. Kalyanaraman B, Dranka BP, Hardy M, Michalski R, Zielonka J. HPLC-based monitoring of products formed from hydroethidine-based fluorogenic probes—the ultimate approach for intra- and extracellular superoxide detection. *Biochim Biophys Acta*. 2014;1840:739–44. [PubMed: 23668959]
43. Robinson KM, Janes MS, Pehar M, Monette JS, Ross MF, Hagen TM, et al. Selective fluorescent imaging of superoxide in vivo using ethidium-based probes. *Proc Natl Acad Sci USA*. 2006;103:15038–43. [PubMed: 17015830]
44. Murphy MP. How mitochondria produce reactive oxygen species. *Biochem J*. 2009;417:1–13. [PubMed: 19061483]
45. Bleier L, Drose S. Superoxide generation by complex III: from mechanistic rationales to functional consequences. *Biochim Biophys Acta*. 2013;1827:1320–31. [PubMed: 23269318]
46. Wong HS, Dighe PA, Mezera V, Monternier PA, Brand MD. Production of superoxide and hydrogen peroxide from specific mitochondrial sites under different bioenergetic conditions. *J Biol Chem*. 2017;292:16804–9. [PubMed: 28842493]
47. Daiber A, Di Lisa F, Oelze M, Kröller-Schön S, Steven S, Schulz E, et al. Crosstalk of mitochondria with NADPH oxidase via reactive oxygen and nitrogen species signalling and its role for vascular function. *Br J Pharm*. 2017;174:1670–89.
48. Li H, Han W, Villar VA, Keever LB, Lu Q, Hopfer U, et al. D1-like receptors regulate NADPH oxidase activity and subunit expression in lipid raft microdomains of renal proximal tubule cells. *Hypertension*. 2009;53:1054–61. [PubMed: 19380616]
49. Yang S, Yang Y, Yu P, Yang J, Jiang X, Villar VA, et al. Dopamine D1 and D5 receptors differentially regulate oxidative stress through paraoxonase 2 in kidney cells. *Free Radic Res*. 2015;49:397–410. [PubMed: 25740199]
50. Sulaiman D, Li J, Devarajan A, Cunningham CM, Li M, Fishbein GA, et al. Paraoxonase 2 protects against acute myocardial ischemia-reperfusion injury by modulating mitochondrial function and oxidative stress via the PI3K/Akt/GSK-3 β RISK pathway. *J Mol Cell Cardiol*. 2019;129:154–64. [PubMed: 30802459]
51. Li Z, Ji X, Wang W, Liu J, Liang X, Wu H, et al. Ammonia induces autophagy through dopamine receptor D3 and mTOR. *PLoS ONE*. 2016;11:e0153526. [PubMed: 27077655]
52. Shin JH, Park SJ, Kim ES, Jo YK, Hong J, Cho DH. Sertindole, a potent antagonist at dopamine D2 receptors, induces autophagy by increasing reactive oxygen species in SH-SY5Y neuroblastoma cells. *Biol Pharm Bull*. 2012;35:1069–75. [PubMed: 22791154]
53. Yan H, Li WL, Xu JJ, Zhu SQ, Long X, Che JP. D2 dopamine receptor antagonist raclopride induces non-canonical autophagy in cardiac myocytes. *J Cell Biochem*. 2013;114:103–10. [PubMed: 22886761]
54. Dolma S, Selvadurai HJ, Lan X, Lee L, Kushida M, Voisin V, et al. Inhibition of dopamine receptor D4 impedes autophagic flux, proliferation, and survival of glioblastoma stem cells. *Cancer Cell*. 2016;29:859–73. [PubMed: 27300435]
55. Jose PA, Eisner GM, Drago J, Carey RM, Felder RA. Dopamine receptor signaling defects in spontaneous hypertension. *Am J Hypertens*. 1996;9:400–5. [PubMed: 8722444]
56. Missale C, Nash SR, Robinson SW, Jaber M, Caron MG. Dopamine receptors: from structure to function. *Physiol Rev*. 1998;78:189–225. [PubMed: 9457173]
57. Gildea JJ, Shah I, Weiss R, Casscells ND, McGrath HE, Zhang J, et al. HK-2 human renal proximal tubule cells as a model for G protein-coupled receptor kinase type 4-mediated dopamine 1 receptor uncoupling. *Hypertension*. 2010;56:505–11. [PubMed: 20660820]
58. Lee J, Giordano S, Zhang J. Autophagy, mitochondria and oxidative stress: cross-talk and redox signalling. *Biochem J*. 2012;441:523–40. [PubMed: 22187934]

59. Pyo JO, Nah J, Kim HJ, Lee HJ, Heo J, Lee H, et al. Compensatory activation of ERK1/2 in Atg5-deficient mouse embryo fibroblasts suppresses oxidative stress-induced cell death. *Autophagy*. 2008;4:315–21. [PubMed: 18196969]
60. Tian Y, Kuo CF, Sir D, Wang L, Govindarajan S, Petrovic LM, et al. Autophagy inhibits oxidative stress and tumor suppressors to exert its dual effect on hepatocarcinogenesis. *Cell Death Differ*. 2015;22:1025–34. [PubMed: 25526090]
61. Diakopoulos KN, Lesina M, Wormann S, Song L, Aichler M, Schild L, et al. Impaired autophagy induces chronic atrophic pancreatitis in mice via sex- and nutrition-dependent processes. *Gastroenterology*. 2015;148:626–38. [PubMed: 25497209]
62. Harada S, Nakagawa T, Yokoe S, Edogawa S, Takeuchi T, Inoue T, et al. Autophagy deficiency diminishes indomethacin-induced intestinal epithelial cell damage through activation of the ERK/Nrf2/HO-1 pathway. *J Pharm Exp Ther*. 2015;355:353–61.
63. Jones DC, Gunasekar PG, Borowitz JL, Isom GE. Dopamine-induced apoptosis is mediated by oxidative stress and is enhanced by cyanide in differentiated PC12 cells. *J Neurochem*. 2000;74:2296–304. [PubMed: 10820189]
64. Leng ZG, Lin SJ, Wu ZR, Guo YH, Cai L, Shang HB, et al. Activation of DRD5 (dopamine receptor D5) inhibits tumor growth by autophagic cell death. *Autophagy*. 2017;13:1404–19. [PubMed: 28613975]
65. Yadav A, Vallabu S, Arora S, Tandon P, Slahan D, Teichberg S, et al. Ang II promotes autophagy in podocytes. *Am J Physiol Cell Physiol*. 2010;299:C488–96. [PubMed: 20484657]
66. Sachse A, Wolf G. Angiotensin II-induced reactive oxygen species and the kidney. *J Am Soc Nephrol*. 2007;18:2439–46. [PubMed: 17687073]
67. Zeng C, Yang Z, Wang Z, Jones J, Wang X, Altea J, et al. Interaction of angiotensin II type 1 and D5 dopamine receptors in renal proximal tubule cells. *Hypertension*. 2005;45:804–10. [PubMed: 15699451]
68. Haller M, Hock AK, Giampazolias E, Oberst A, Green DR, Debnath J, et al. Ubiquitination and proteasomal degradation of ATG12 regulates its proapoptotic activity. *Autophagy*. 2014;10:2269–78. [PubMed: 25629932]
69. Jiang S, Park DW, Gao Y, Ravi S, Darley-Usmar V, Abraham E, et al. Participation of proteasome-ubiquitin protein degradation in autophagy and the activation of amp-activated protein kinase. *Cell Signal*. 2015;27:1186–97. [PubMed: 25728513]
70. Livnat-Levanon N, Glickman MH. Ubiquitin-proteasome system and mitochondria - reciprocity. *Biochim Biophys Acta*. 2011;1809:80–7. [PubMed: 20674813]
71. Omar B, Zmuda-Trzebiatowska E, Manganiello V, Göransson O, Degerman E. Regulation of AMP-activated protein kinase by cAMP in adipocytes: roles for phosphodiesterases, protein kinase B, protein kinase A, Epac and lipolysis. *Cell Signal*. 2009;21:760–6. [PubMed: 19167487]
72. Decara J, Rivera P, Arrabal S, Vargas A, Serrano A, Pavón FJ, et al. Cooperative role of the glucagon-like peptide-1 receptor and β 3-adrenergic-mediated signalling on fat mass reduction through the downregulation of PKA/AKT/AMPK signalling in the adipose tissue and muscle of rats. *Acta Physiol*. 2018;222:e13008.
73. Valsecchi F, Ramos-Espiritu LS, Buck J, Levin LR, Manfredi G. cAMP and mitochondria. *Physiology*. 2013;28:199–209. [PubMed: 23636265]
74. Torres-Quiroz F, Filteau M, Landry CR. Feedback regulation between autophagy and PKA. *Autophagy*. 2015;11:1181–3. [PubMed: 26046386]
75. Lee YJ, Shu MS, Kim JY, Kim YH, Sim KH, Sung WJ, et al. Cilostazol protects hepatocytes against alcohol-induced apoptosis via activation of AMPK pathway. *PLoS ONE*. 2019;14:e0211415. [PubMed: 30695051]
76. Chen ML, Yi L, Jin X, Liang XY, Zhou Y, Zhang T, et al. Resveratrol attenuates vascular endothelial inflammation by inducing autophagy through the cAMP signaling pathway. *Autophagy*. 2013;9:2033–45. [PubMed: 24145604]
77. Akabane S, Uno M, Tani N, Shimazaki S, Ebara N, Kato H, et al. PKA regulates PINK1 stability and parkin recruitment to damaged mitochondria through phosphorylation of MIC60. *Mol Cell*. 2016;62:371–84. [PubMed: 27153535]

78. Wolter S, Kloth C, Golombek M, Dittmar F, Försterling L, Seifert R. cCMP causes caspase-dependent apoptosis in mouse lymphoma cell lines. *Biochem Pharm.* 2015;98:119–31. [PubMed: 26300059]
79. Yu P, Sun M, Villar VA, Zhang Y, Weinman EJ, Felder RA, et al. Differential dopamine receptor subtype regulation of adenylyl cyclases in lipid rafts in human embryonic kidney and renal proximal tubule cells. *Cell Signal.* 2014;26:2521–9. [PubMed: 25049074]

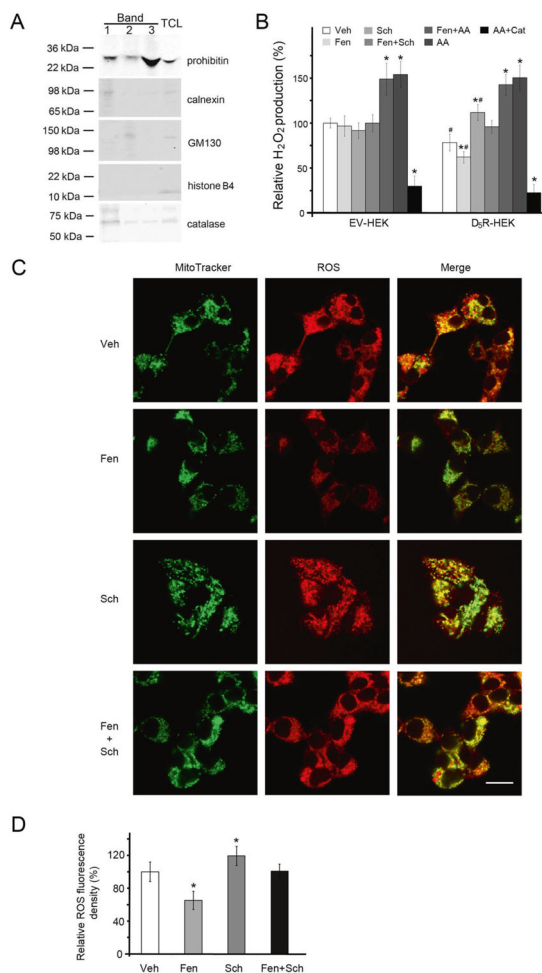


Fig. 1. Mito-ROS production in D₅R-HEK293 cells. **A** Characterization of purified mitochondria (Band 3, as described in Supplementary Fig. 7) by immunoblotting with antibodies against markers for mitochondria (prohibitin), endoplasmic reticula (calnexin), Golgi bodies (GM130), nuclei (histone B4), and peroxisomes (catalase). TCL total cell lysate. **B** H₂O₂ production in isolated mitochondria, with pyruvate (5 mM) and malate (5 mM) as the substrates. Veh vehicle, Fen fenoldopam (D₁R/D₅R agonist, 1.0 μM, 12 h), Sch Sch23390 (D₁R/D₅R antagonist 1.0 μM, 12 h), AA antimycin A (Qi site inhibitor of mitochondrial ETC Complex III, 0.75 μM, 2 h), Cat catalase (10 μM, 30 min prior to AA treatment). Open rectangles, empty vector-transfected HEK293 (EV-HEK) cells; filled rectangles, D₅R-overexpressing HEK293 (D₅R-HEK) cells. $n = 4/\text{group}$, $*P < 0.05$ vs Veh, $\#P < 0.05$ vs EV-HEK. **C** D₅R-HEK293 cells were treated with Veh or Fen (1.0 μM, 12 h) in the absence or presence of Sch (1.0 μM, 12 h). Mitochondria were stained with MitoTracker Green; mito-ROS were monitored with MitoSOX Red. Bar, 20 μm. The images are from one of three independent experiments. **D** The MitoSOX Red fluorescence density was obtained in 3–5 random fields from 25–40 D₅R-HEK293 cells in three independent experiments, as described in **C**; $*P < 0.05$ vs Veh

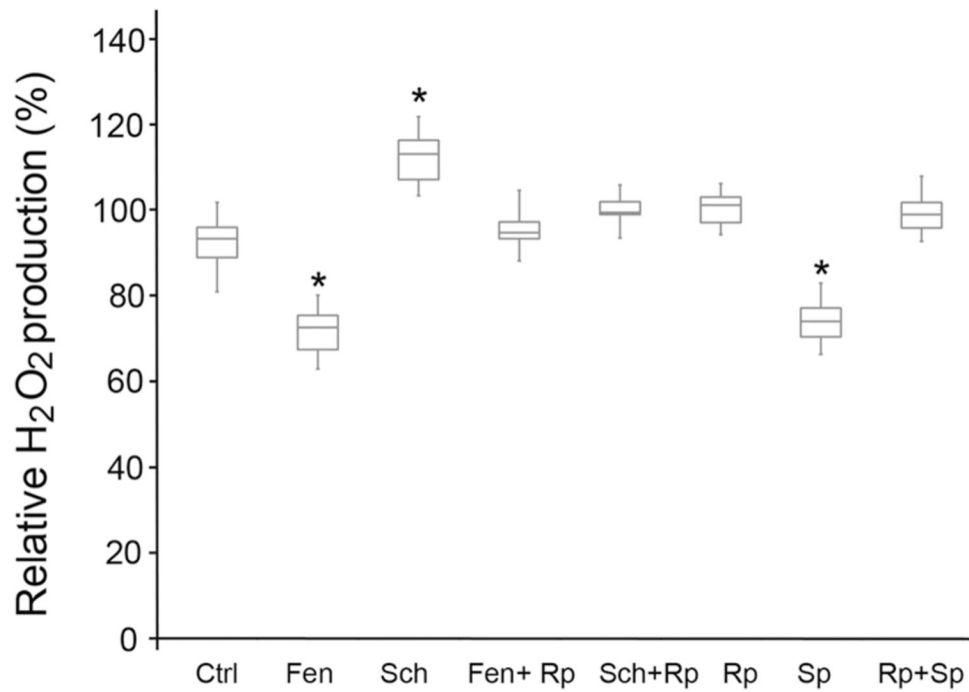


Fig. 2. cAMP dependence of D₅R-mediated inhibition of mito-ROS production. D₅R-HEK293 cells were preincubated for 30 min with vehicle (Ctrl), Fen (fenoldopam, D₁R/D₅R agonist, 1.0 μM), Sch (Sch23390, D₁R/D₅R antagonist, 1.0 μM), Fen + Rp (Rp-cAMPS, PKA inhibitor, 50 μM), Sch + Rp, Rp alone, Sp (Sp-cAMPS, PKA activator, 10 μM) alone, or Rp + Sp. *n* = 6/group, **P* < 0.05 vs Ctrl

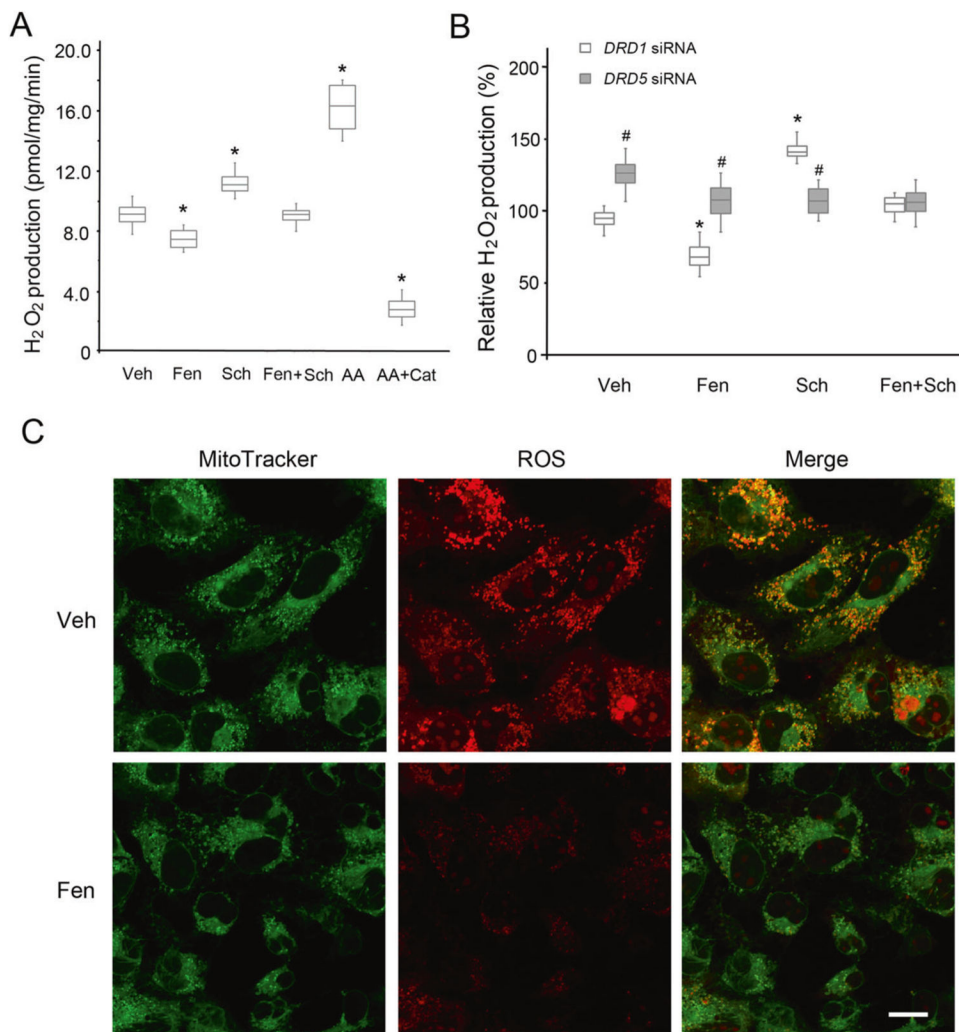


Fig. 3. Mito-ROS production in human RPT cells. **A** H₂O₂ production from mitochondria isolated from human RPT cells, with pyruvate and malate as the substrates. Veh vehicle, Fen fenoldopam (D₁R/D₅R agonist, 1.0 μM, 12 h), Sch Sch23390 (D₁R/D₅R antagonist, 1.0 μM, 12 h), AA antimycin A (Qi site inhibitor of mitochondrial ETC Complex III, 0.75 μM, 2 h), Cat catalase (10 μM, 30 min prior to AA treatment). *n* = 4/group, **P* < 0.05 vs Veh. **B** H₂O₂ production from mitochondria isolated from *DRD1*- or *DRD5*-silenced human RPT cells. The cells were treated with vehicle (Veh), Fen (1.0 μM, 12 h), or Sch (1.0 μM, 12 h). *n* = 4/group, **P* < 0.05 vs Veh, #*P* < 0.05 vs *DRD1*-silenced RPT cells. **C** Mito-ROS staining in *DRD1*-silenced intact human RPT cells treated with Veh or Fen (1.0 μM, 12 h), as indicated. Bar, 10 μm. The images are from one of three independent experiments

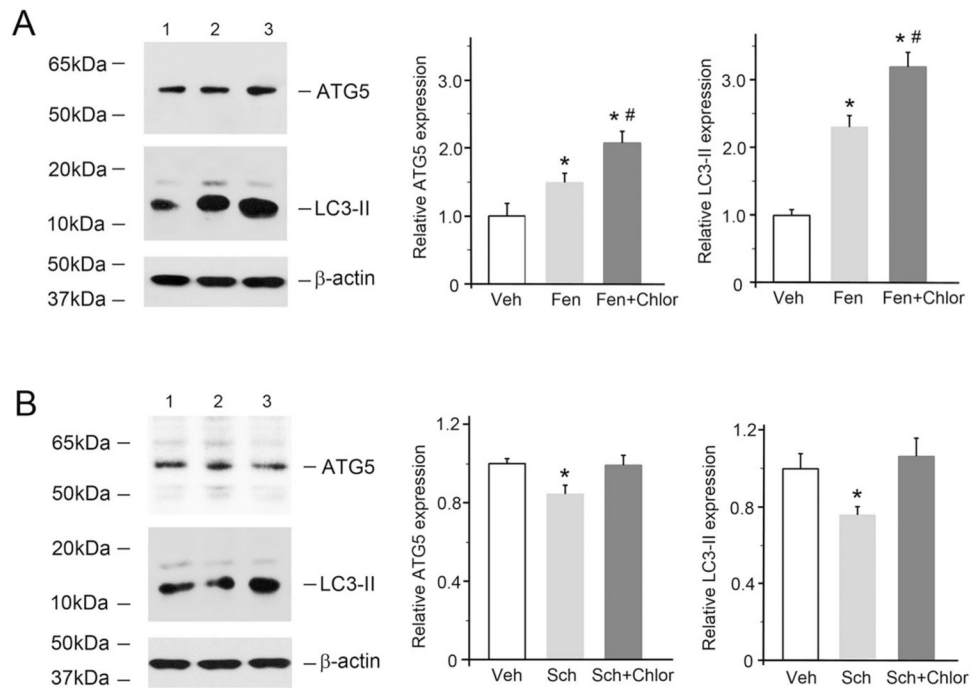


Fig. 4. D₅R-mediated increases in the levels of autophagy-related proteins in D₅R-HEK293 cells. **A** The cells were treated with fenoldopam (Fen, 1.0 μ M, 12 h) in the absence or presence of chloroquine (an inhibitor of autophagosome-lysosome fusion/lysosome-mediated proteolysis, 10 μ M, 12 h). Immunoblots from one of five independent experiments are shown. Lane 1, vehicle (Veh); lane 2, fenoldopam (Fen); lane 3, fenoldopam plus chloroquine (Fen + Chlor). The β -actin protein level was used to measure the amount of sample loaded in each lane. $n = 5/\text{group}$, * $P < 0.05$ vs Veh, # $P < 0.05$ vs Fen. **B** D₅R-HEK293 cells were treated with Sch (Sch23390, 1.0 μ M, 12 h) in the absence or presence of chloroquine (Chlor). Immunoblots from one of five independent experiments are shown. Lane 1, Veh; lane 2, Sch; lane 3, Fen + Chlor. The β -actin protein level was used to measure the amount of sample loaded in each lane. $n = 5/\text{group}$, * $P < 0.05$ vs others

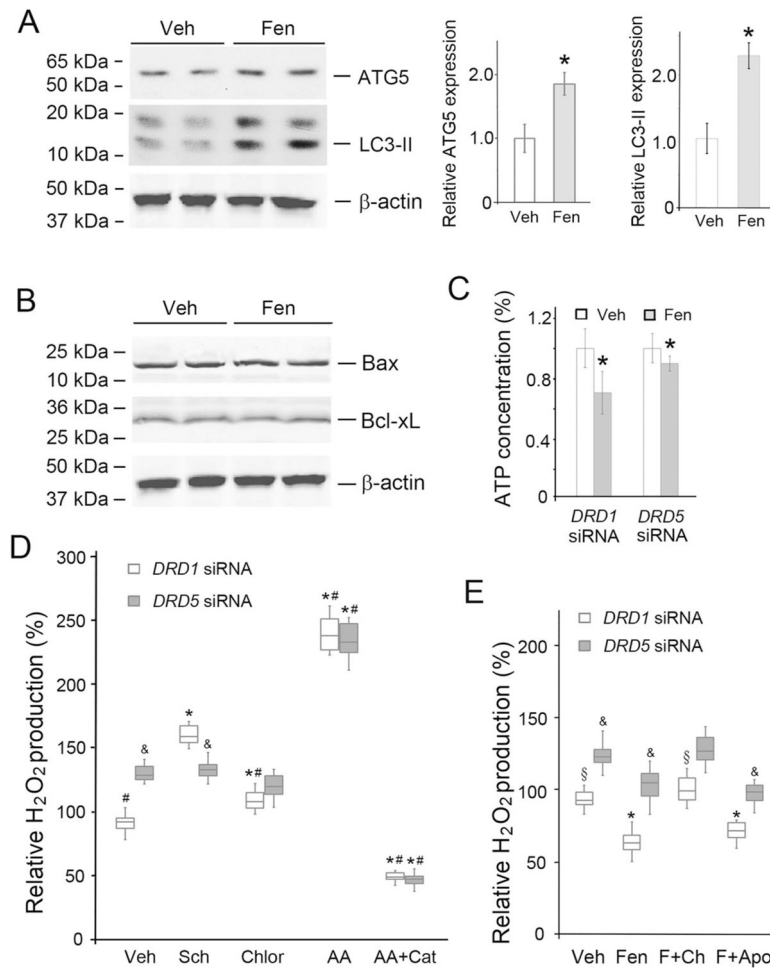


Fig. 5. D₅R-mediated alteration of autophagy-related protein expression and function. **A** Autophagy marker protein expression in *DRD1*-silenced human RPT cells treated with Veh (vehicle) or Fen (fenoldopam, 1.0 μ M, 12 h). The immunoblots show that the levels of the autophagy marker proteins ATG5 and LC3-II increased with Fen treatment. $n = 4$ /group, * $P < 0.05$ vs Veh. **B** Proapoptotic and antiapoptotic protein (Bax and Bcl-xL) expression in *DRD1*-silenced human RPT cells. The human RPT cells were treated, as described in **A**. **C** ATP concentrations were measured using a bioluminescence assay kit (Roche). The ATP concentration in human RPT cells treated with vehicle was set to 1. Veh vehicle, Fen fenoldopam (1.0 μ M, 12 h). $n = 5$ /group, * $P < 0.05$ vs Veh. **D** H₂O₂ production in isolated mitochondria from *DRD1*- or *DRD5*-silenced human RPT cells treated as indicated. Veh vehicle, Sch Sch23390 (1.0 μ M, 12 h), Chlor chloroquine (inhibitor of autophagosome-lysosome fusion/lysosome-mediated proteolysis, 10 μ M, 12 h), AA antimycin A (Qi site inhibitor of mitochondrial ETC Complex III, 0.75 μ M, 2 h), Cat catalase (10 μ M, 30 min prior to AA treatment). $n = 5$ –6/group, * $P < 0.05$ vs Veh, # $P < 0.05$ vs Sch, & $P < 0.05$ vs *DRD1* siRNA. **E** H₂O₂ production in isolated mitochondria from human RPT cells, as described in **D**. Veh vehicle, Fen or F fenoldopam (1.0 μ M, 12 h), Ch chloroquine (10 μ M, 12 h), Apo apocynin A (10 μ M, 12 h). $n = 8$ /group, * $P < 0.05$ vs Veh, § $P < 0.05$ vs Fen, & P

< 0.05 vs *DRD1* siRNA. There was no significant difference between the Fen and Fen + Apo groups in terms of human RPT cells lacking D₁R (*DRD1* siRNA) or D₅R (*DRD5* siRNA)

Author Manuscript

Author Manuscript

Author Manuscript

Author Manuscript

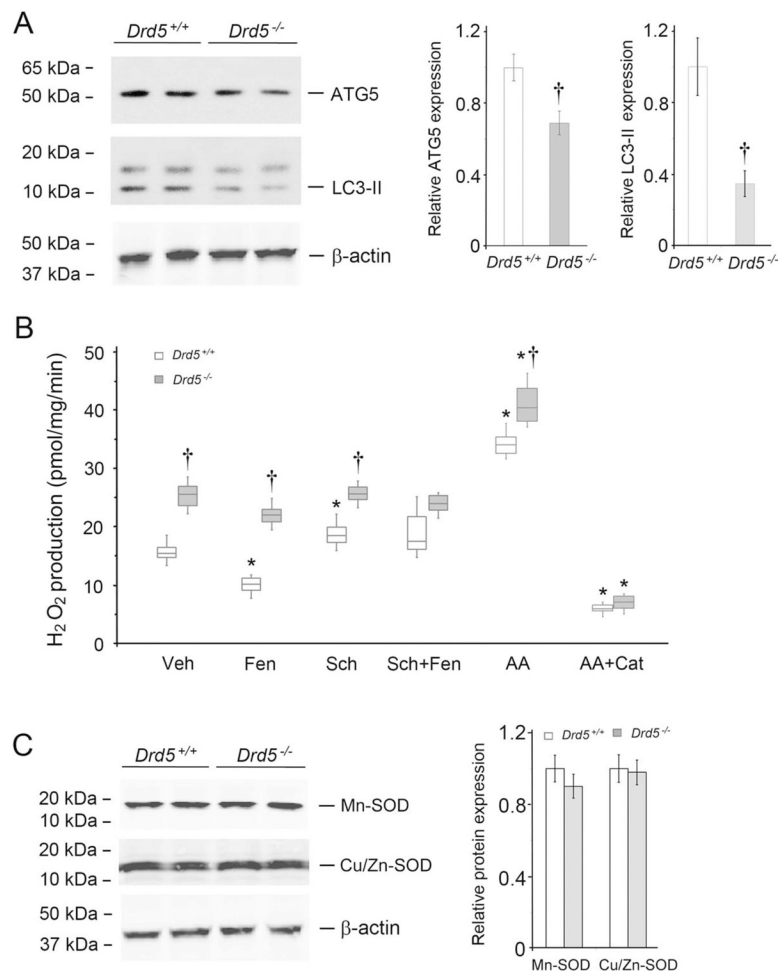


Fig. 6. Autophagy protein expression and mito-ROS production in mouse kidney cortices. **A** Autophagy marker protein expression in kidney cortices of *Drd5*^{-/-} mice and their wild-type (*Drd5*^{+/+}) littermates. The immunoblots show decreased protein expression of the autophagy marker proteins ATG5 and LC3-II in the kidney cortices of *Drd5*^{-/-} mice relative to *Drd5*^{+/+} littermates. $n = 4/\text{group}$, $^{\dagger}P < 0.05$ vs *Drd5*^{+/+}. **B** H₂O₂ production in isolated mitochondria from kidney cortices of *Drd5*^{-/-} mice and their *Drd5*^{+/+} littermates. Veh vehicle, Fen fenoldopam (1.0 μM , 12 h), Sch Sch23390 (1.0 μM , 12 h), AA antimycin A (0.75 μM , 2 h), Cat catalase (10 μM , 30 min prior to AA treatment). $n = 6/\text{group}$, $*P < 0.05$ vs Veh, $^{\dagger}P < 0.05$ vs *Drd5*^{+/+}. **C** Mitochondrial superoxide dismutase (SOD) protein (Mn-SOD and Cu/Zn-SOD) expression in isolated mitochondria from kidney cortices of *Drd5*^{-/-} mice and their *Drd5*^{+/+} littermates. $n = 4/\text{group}$. There were no significant differences in SOD protein expression between *Drd5*^{+/+} and *Drd5*^{-/-} mice